

Fractography of Fatigue Cracks in Aluminium Alloy AA7050 Subjected to Interrupted Ageing and Retro-Ageing Heat Treatments

André L. M. Carvalho, Juliana P. Martins, Enrico Salvati, Tan Sui, Alexander M. Korsunsky*

Abstract— Novel heat treatments for aerospace aluminium alloys allow simultaneous improvements of ductility and strength. In the present study we consider the effects of retro-ageing and interrupted heat treatments of aluminium alloy AA7050 on its fatigue behaviour, including the consequences of crack closure for fatigue crack growth rate. SEM fractography is used to visualise striations associated with crack front advance in individual cycles, and a correlation is made with the overall crack growth rate, and the conditions of crack propagation.

Index Terms — Aluminium alloy, ageing treatment, fractography, fatigue crack

I. INTRODUCTION

Reductions in weight have always been a major criterion for the selection of materials for aerospace applications. This led to the development of various high strength aluminum alloys during the last half a century [1]. The key role of the 7050-T7451 aluminum alloy plate have been extensively used for manufacturing of aircraft structural components due to their high strength, low density, excellent hot workability, fracture toughness and fatigue resistance [2]. Moreover, the overageing heat treatment T7451 has been traditionally applied to reduce the susceptibility of commercial Al-7075-T651 alloy to stress corrosion cracking (SCC). However, this heat treatment necessarily leads to a sacrifice of the maximum strength of this alloy [3]. Accordingly, multiple-stage ageing treatments have been developed for aluminum alloys to further enhance the mechanical property response, [4]. In

order to improve the compromise between mechanical strength and corrosion resistance, it has been proposed to replace the traditional two-step heat treatment of these alloys by a three-step heat treatment, called retrogression and re-ageing (RRA) treatment [5].

Recent experimental studies have reported new heat treatment schedules (designated T6I4, I=interrupted) that, when applied to Al alloys, offer the possibility of avoiding the inverse correlations between some of the important mechanical properties, such as yield strength and elongation, and yield strength and fracture toughness [6].

Among the aging technologies, interrupted multi-step aging attracts much attention, which may lead to simultaneous increase in both tensile and fracture toughness of a wide range of aging- hardening aluminum alloys [7]

These observations have received much attention from both industry (who are interested in creating new property profiles for existing alloys) and academia (because of modifying the size, morphology and distribution of particles in aged aluminum alloys are not deeply understood);

However, few studies have referred to T6I4 and RRA-treated 7050 alloy in order to explore the potential of multistage ageing treatments on the fatigue nucleation and crack growth behavior.

The purpose of this study is investigate in details the influence of T6I4-65 and RRA ageing treatments to produce different combinations of tensile properties on the fatigue crack growth rate and fracture behaviors. It was applied single overload to evaluation its influence at the retardation fatigue crack growth rate and fracture process.

II. EXPERIMENTAL PROCEDURE

A. Material

The material used in the present study was a 7050-T7451 aluminium alloy plate of 3" (76.8mm) thickness and the composition (in wt%) of "5.58Zn, 1.88Mg, 2.00Cu, 0.07Fe, 0.02Si, 0.15Zr, Al balance", provided by the Embraer Company. All specimens were removed from the longitudinal (LD) to rolling direction. Tensile properties of the material in the T7451, T6I4-65 and RRA conditions such as: the ultimate tensile strength (UTS), the yield strength and the reduction in area, respectively, are shown in Table I. It is worth noting that the RRA condition gives

Manuscript received January 05, 2016; revised January 10, 2016. This work was supported in part by the CAPES under Grant BEX 2606/15-1 and BEX 2638/15-0. AMK acknowledges funding received for the MBLEM laboratory at Oxford through EU FP7 project iSTRESS (604646).

A. L. M. Carvalho is with Department of Material Engineering, State University of Ponta Grossa, PR, Brazil, 84030-900 (andreilmc@uepg.br).

J. P. Martins is with Department of Chemical Engineering, Federal University of Technology-Paraná, 84016-210 (julianamartins@utfpr.edu.br).

E. Salvati is with Department of Engineering Science, University of Oxford, U.K, OX1 3PJ (enrico.salvati@eng.ox.ac.uk).

T. Sui is with Department of Engineering Science, University of Oxford, U.K, OX1 3PJ (tan.sui@eng.ox.ac.uk).

A. M. Korsunsky is Head of MBLEM (Multi-Beam Laboratory for Engineering Microscopy), Department of Engineering Science, University of Oxford, U.K, OX1 3PJ (alexander.korsunsky@eng.ox.ac.uk).

* Corresponding author

tensile properties superior to the T7451 condition, whereas the T6I4-65 condition has a decrease of “19.46%” in the yield strength compared to the as-received T7451 condition.

Table I. Tensile properties results from the T7451, T6I4-65 and RRA conditions.

Condition	YS (MPa)	UTS(MPa)	R.A. (%)
T7451	492 ± 10.5	592 ± 23	3.7 ± 1.2
T6I4-65	452 ± 10.3	534 ± 14.5	38.17 ± 2.9
RRA	540 ± 15.5	613.20 ± 4.8	22.79 ± 3.2

B. Heat Treatment

Two types of heat treatment were considered in the present study, carried out according to the following schedules. The first, denoted the T6I4-65 condition, was solution treated at “485 °C for 4 h”, water quenched, ageing was interrupted at “130 °C for 15 min”, followed by ageing at “65°C for two months”. The second, denoted the RRA condition, was solution treated at “485 °C for 4 h”, water quenched, and aged at “130°C for 24h” followed by retrogression at “185°C for 20 min”, followed by ageing at “65°C for two months”. The other condition considered for reference was the as-received T7451 condition.

C. Fatigue Fracture Surface Analysis

Fractography analysis of fatigue crack surfaces was carried out at the locations of crack growth in the near-threshold, low and high ΔK regimes, as also at the rupture regime, for the T7451, T6I4-65, and RRA conditions. All fracture analysis has been performed at the Tescan FIB/SEM LIRA3XM using secondary electron mode.

Fatigue crack propagation testing was performed under constant stress amplitude using a servohydraulic “15 kN” fatigue machine on compact tension (CT) specimens (Fig 1), with plate width “W=50 mm” and thickness “9.5 mm” machined from the plate with L-T orientation, with the crack growth aligned with the transverse direction. All samples were pre-cracked as described in ASTM E 647 -05 [8]. The frequency of “10 Hz” and stress ratio of “R = 0.1” were used for testing. Crack length was measured from the digital camera attached to Questar long range telescope. A single overload (OL) of 50% was applied to evaluate its influence on the retardation of fatigue crack growth rate and the subsequent crack propagation process.

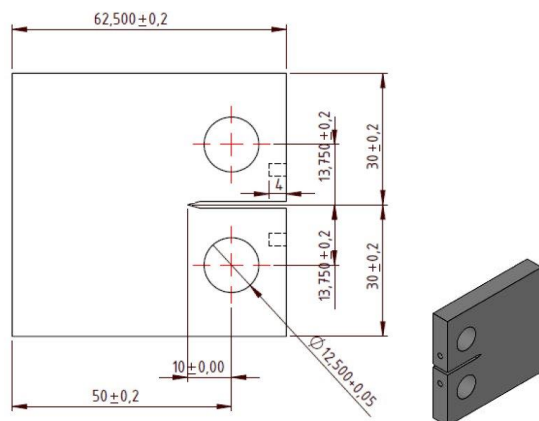


Fig 1. Geometry of the C(T) specimen (dimensions in mm).

III. RESULTS AND DISCUSSION

A. Fracture Surface Analysis

Examination of the surfaces reveals a fractured surface region close to perpendicular to the principal applied load, accompanied by shear fracture at specimen edges. In the three conditions tested, double shear lips were evident along the fracture path. The crack extension mechanism depends on the crack driving force that varies between pure Mode I in the main crack, and a mixture of Mode I and Mode II at the shear lips, and at locations of uneven fracture surface within the main crack [9]. The surface roughness was evaluated using a Alicona optical Infinite Focus 3D micro-coordinate measurement equipment for the three conditions in terms of the surface roughness parameter R_s according to the ASM Handbook [10]. R_s is the ratio $R_s = S_t/A$ given from the true surface area S_t divided by the projected area A . As shown in Fig 2, the T7451 condition reveals higher R_s values measured along at chosen segments corresponding to similar crack growth position for the three conditions investigated. The average values measured were 1.23 for T7451, 1.15 for, T6I4-65, and 1.19 for RRA, respectively (Fig 2).

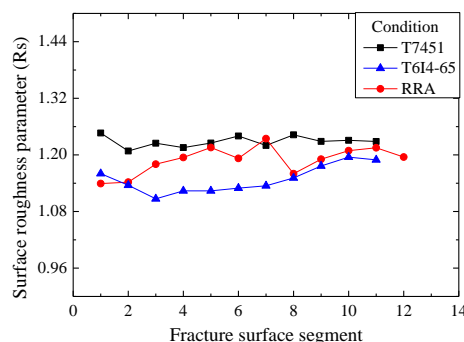


Fig 2. Surface roughness parameter from the three conditions.

In the experimental results reported in [11] on the aluminium alloy showed increase crack growth resistance of the plate was attributed two factors: i) a lower ductility in relation to other higher ductility and ii) a pronounced crack closure at crack path promoted by higher surface roughness. In the present study, the T7451 condition showed higher surface roughness (Fig 2), but also lower ductility compared other two conditions. This suggests the significance of roughness-induced crack closure amongst different crack retardation mechanisms for this condition.

B. Near-threshold regime

Fig 3 a-c shows the SEM fractographs of the fatigue crack growth specimens tested at the near-threshold regime. It can be seen that crack growth occurs on multiple facets at different angles with respect to each other for all three conditions studied. The propensity for the formation of facets is more evident in the RRA condition in which the features also appear larger than in the T6I4-65 and T7451 conditions. In Fig 3c, changes in the orientation of facets

can be noted (indicated by black arrows), likely to be associated with the crack path crossing a grain boundary.

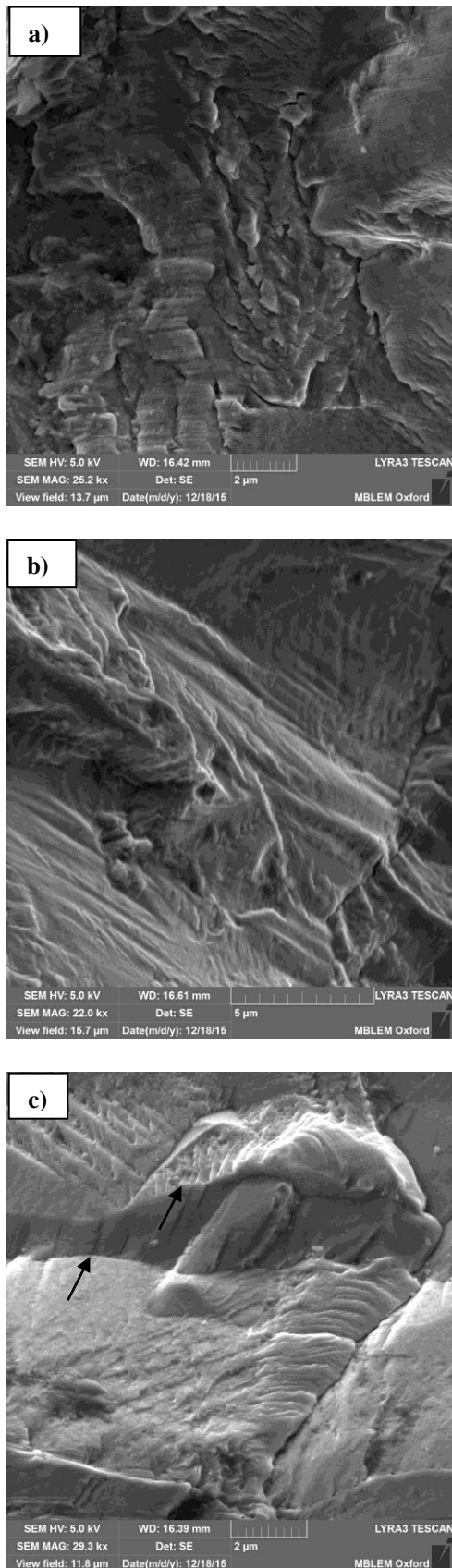


Fig 3. SEM fractographs in the near-threshold regime of the alloy in the three conditions (a) T7451 and (b) T614-65 and (c) RRA (crack propagation direction is from left to right).

C. Low ΔK regime

The results of the examination of the fracture surfaces conducted in the low ΔK regime can be seen in Fig 4 a-c. For the T7451 condition (Fig 4a), the formation of deep pockets is noticeable, as also is the absence of facets.

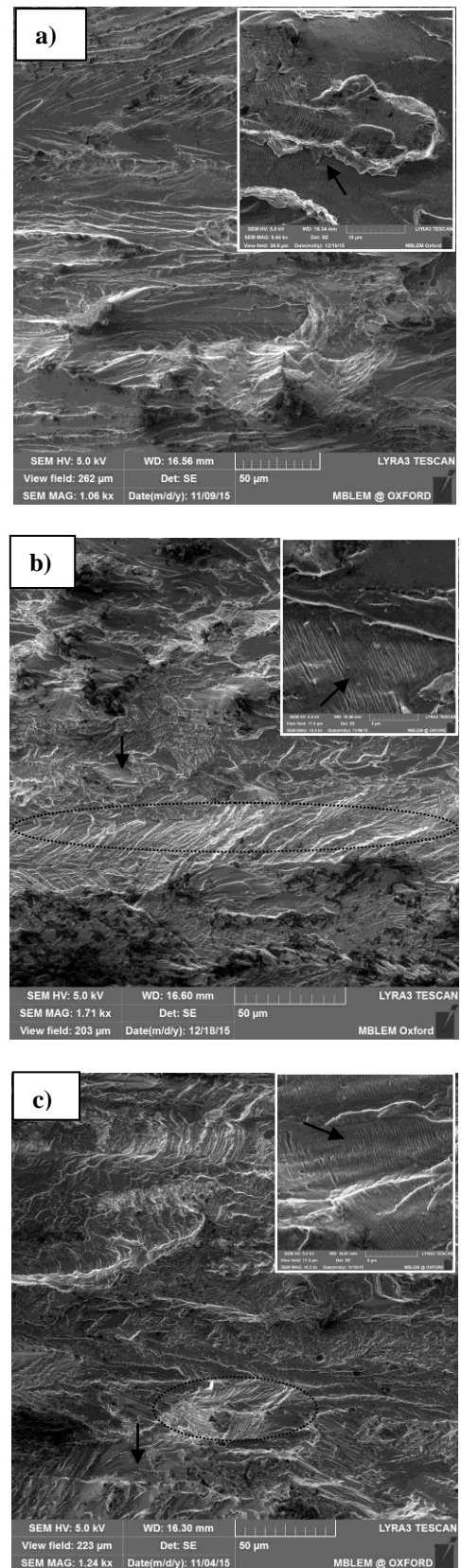


Fig 4. SEM fractographs in the Paris growth regime (Low ΔK level) of the alloy in three conditions (a) T7451, (b) T614-65 and (c) RRA (crack propagation direction is from left to right).

In contrast, the T6I4-65 and RRA conditions (Fig 4b-c) has shown some different features present at the fracture surface, such as shallow pockets, a predominance of small flat facets (indicated by the black arrows), and the small and large facets containing multiple wavy regions encircled using dashed lines. Moreover, for all three conditions it is possible to notice the presence secondary cracks. Void formation at the coarse grain boundary is also observed, except for the RRA condition.

D. Overload region

Fig 5 a-c shows SEM fractographs focused at the location of the overload. The purpose of this examination was to consider the arrangement of crack growth striations following propagation beyond the overload region in the alloy in three conditions. The appearance of striations across the fractured surface was tortuous for the T7451, T6I4-65 and RRA conditions, with the spacing in the range “3.94-9.05 μm ”, “14.82-17.63 μm ” and “30.68-34.65 μm ”, respectively. In Fig 5 a-c it is also possible to observe narrow flat facets for the T7451 condition, while for both T6I4-65 and RRA conditions multiple large flat facet were observed.

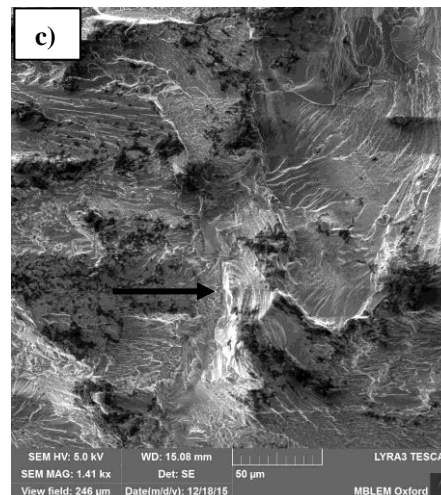
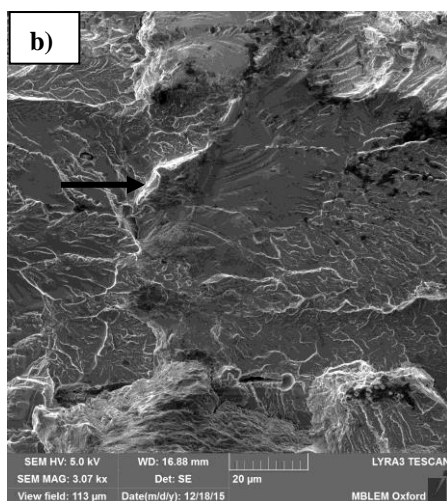
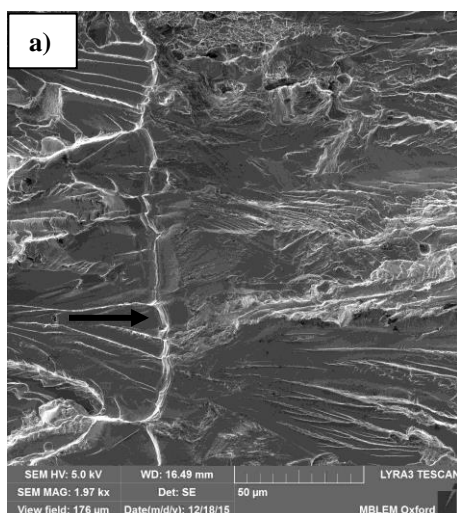
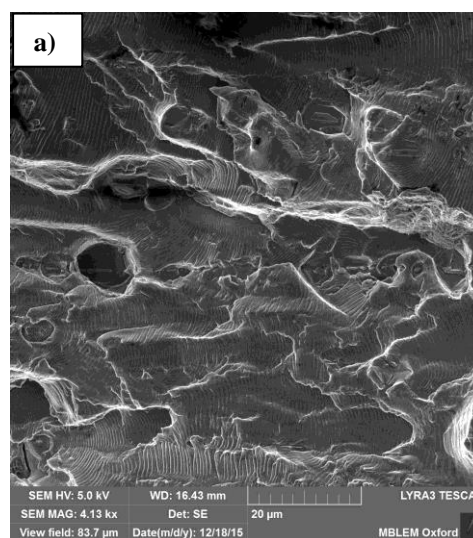


Fig 5. SEM fractographs at the striation region after overload of the alloy in three conditions (a) T7451, (b) T6I4-65 and (c) RRA (crack propagation direction is from left to right).

E. High ΔK regime

The fractographs collected from the region of crack growth in the high ΔK regime can be seen in Fig 6 a-c, and reveal the following features. For the T7451 condition, apart from the absence of facets, similar features to the low ΔK regime can be recognised, but their prominence is greater due to the high ΔK . The same features seen in the low ΔK regime for both T6I4-65 and RRA conditions were also observed in this regime. It is possible to notice in Fig 6b-c the orientation of striation alignment differs from patch to patch. This suggests that the crack front and the crack growth direction are changing in the course of propagation, i.e. the crack front is probably not maintained as a straight line, but is likely to be tortuous. Moreover, for the RRA condition, prominent void formation was observed that is likely to be associated with the crack crossing grain boundaries.



crack growth rate, as shown in Table III.

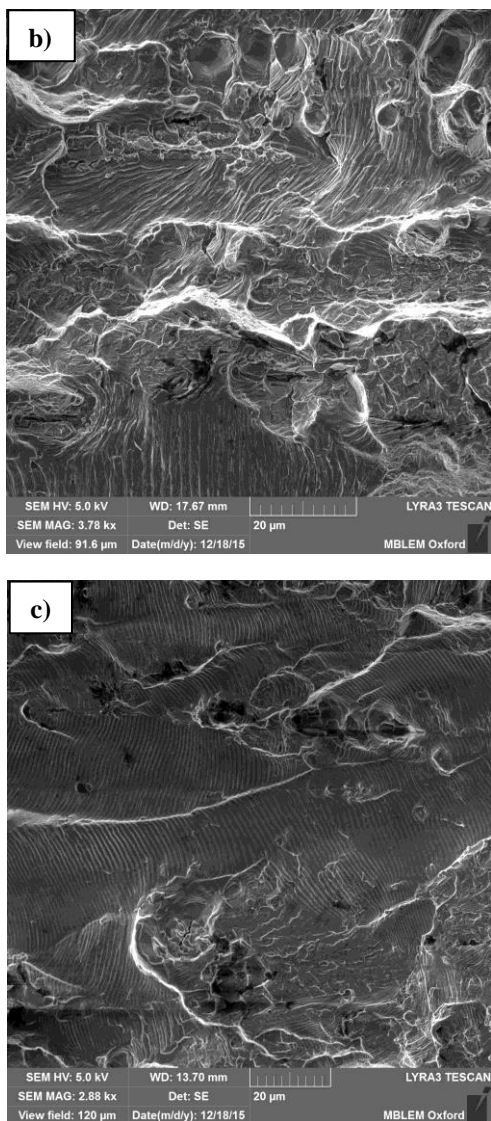


Fig 6 SEM fractographs in the Paris growth regime (high ΔK) of the alloy in three conditions show; (a) for the T7451 the absence of facets, for both (b) T6I4-65 and (c) RRA different striation alignment orientation (crack propagation direction is from left to right).

F. Rupture regime

In the fatigue rupture region, for the T7451, T6I4-65 and RRA conditions, fractographic features can be seen in Fig 7(a-c). Predominantly ductile fracture surfaces were observed, characterised by the large dimples of the order of “2.5–9.5 μm”, “2.2-17.4 μm” and “2.0-12.0 μm” in diameter, respectively. Aggregates of secondary particles could often be seen within these dimples. For the three conditions, intergranular failure along grain boundaries in the fracture surface can be found, with the failure mode being predominantly transgranular. For all regimes investigated for the three conditions, meandering crack surface morphology was always observed.

From the results reported in the literature it is well known that the spacing between adjacent striations correlates with the average crack growth rate per cycle for cyclic loads [3]. Consequently, the data displayed in Table II for the measured striation spacing at the fractured surface for the three conditions suggests a correlation with fatigue

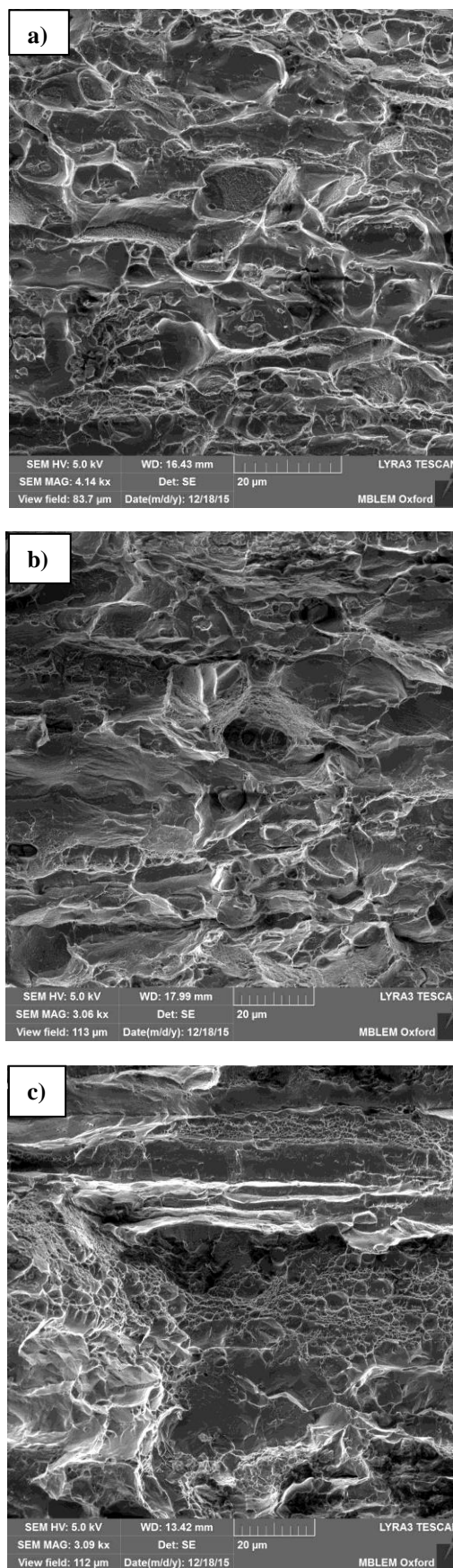


Fig 7. SEM fractographs in rupture regime of the alloy in three conditions (a)T7451, T6I4-65 (b) and (c) RRA (crack propagation direction is from left to right)

From Table II it is possible to note the narrow fatigue striation distance for both RRA and T6I4-65 conditions in low ΔK regime, indicating slow fatigue crack growth rate, i.e. a higher resistance to fatigue crack growth compared to the traditional T7451 condition.

Table II. Experimental results of the measured striation spacing from fractured surface at the different regimes of the three conditions investigated.

Condition	Average striation spacing (μm)			
	Low ΔK	After OL	Moderate ΔK	High ΔK
T7451	0.191	0.128	0.220	0.595
T6I4-65	0.121	0.104	0.151	0.490
RRA	0.097	0.130	0.165	0.485

This behaviour is maintained until in the moderate ΔK regime (corresponding $\Delta K=15$ in Tab.3). It is coincident with the experimental result shown in Table III for the three conditions.

Table III. Fatigue crack growth data of 7050 alloy for the three conditions.

condition	C ($\times 10^{-10}$)	n	da/dN=C(ΔK) ⁿ (m/cycle) ($\times 10^{-7}$)			
			8*	10*	15*	20*
T7451	1.688	2.96	0.80	1.54	5.11	11.98
T6I4-65	0.028	4.46	0.30	0.81	4.93	17.77
RRA	0.003	5.14	0.13	0.41	3.33	14.60

* ΔK =MPa (m)^{0.5}

IV. CONCLUSION

The present study investigated the influence of two types of novel multi-stage heat treatments (T6I4-65 and RRA) on the fractographic appearance of fatigue crack surfaces. The observations were contrasted and compared with the traditional T7451 condition. Fracture analysis was carried out for the near-threshold, low and high ΔK regimes, as well as following the application of a single 50% overload, and for the rupture regime.

The occurrence of uneven areas at the fatigue fracture surface corresponds to crack meandering that increases the total fracture surface and enhances the material resistance to crack propagation. It is surmised that the appearance of crack deflection features is associated with the location of elongated grain boundaries aligned in the longitudinal (rolling) direction of the AA 7050 aluminium alloy. This highlights the importance of mechanical processing and heat treatment conditions for the control of microstructure and mechanical properties of aluminium alloys subjected to complex procedures for the enhancement of performance in aerospace applications.

ACKNOWLEDGMENT

AMK acknowledges access to the facilities at the Research Complex at Harwell (RCaH) granted to the Centre for In situ Processing Studies (CIPS).

REFERENCES

- [1] M. N. Desmukha, R.K. Pandey, A.K. Mukhopadhyay, "Effect of ageing treatments on the kinetics of fatigue crack growth in 7010 aluminium alloy," *Materials Science and Engineering A*, vol. 435-436, pp. 318-326, 2006.
- [2] D. Feng, X.M Zhang, S.D.Liu, T.Wang, Z.Z.Wu, Y.W.Guo, "The effect of pre-ageing temperature and retrogression heating rate on the microstructure and properties of AA7055," *Materials Science & Engineering A*, vol. 588, pp. 34-42, Dec. 2013.
- [3] Y. L. Wang, Q. L. Pan, L. L. Wei, B. Li, Y. Wang, "Effect of retrogression and reaging treatment on the microstructure and fatigue crack growth behavior of 7050 aluminium alloy thick plate," *Materials and Design*, vol. 55, pp. 857-863, Mar. 2014.
- [4] D.D. Risantia, M. Yinb, P.E.J.R.D. del Castillo, S. van der Zwaagc, "A systematic study of the effect of interrupted ageing conditions on the strength and toughness development of AA6061," *Materials Science and Engineering A*, vol. 523, no 1-2, pp. 99-111, Oct. 2009.
- [5] T. Marlaud, A. Deschamps, F. Bley, W. Lefebvre, B. Baroux, "Evolution of precipitate microstructures during the retrogression and re-ageing heat treatment of an Al-Zn-Mg-Cu alloy," *Acta Materialia* vol. 58, no 14, pp. 4814-4826, Aug. 2010.
- [6] M.E. Burba, M.J. Caton, S.K. JHA, and C.J. Szczepanski, "Effect of Aging Treatment on Fatigue Behavior of an Al-Cu-Mg-Ag Alloy," *The Minerals, Metals & Materials Society and ASM International*, vol. 44A, no 11, pp. 4954-4967, Nov. 2013.
- [7] Z. Baohong, X. Baiqing, Z. Yong, Z. Jianbo, W. Feng, and L. Zhihui, "Microstructure and properties characteristic during interrupted multi-step aging in Al-Cu-Mg-Ag-Zr alloy," *RARE METALS*, vol. 30, no. 4, pp. 419-423, Aug. 2011.
- [8] *ASTM Test Methods for Measurement of Fatigue Crack Growth Rates*, ASTM Standard, E 647-95a, 2005.
- [9] P. F. P. de Matos "Plasticity induced fatigue crack closure: Modelling and Experiments," Ph.D. thesis, Dept. Eng. Sci., Oxford Univ., Oxford, UK, 2008.
- [10] *Fractography*, vol. 12, ASM International: the materials information society, USA, 1998, pp. 374-378.
- [11] A.T. Kermanidis and Sp.G. Pantelakis, "Prediction of crack growth following a single overload in aluminum alloy with sheet and plate microstructure," *Engineering Fracture Mechanics* vol. 78, no 11, pp. 2325-2337, July 2011.